CNN-Based Recognition of Liquid–Gas Flow Regimes in a Pipeline Using Gamma-Ray Absorption and Signal Spectrograms*

Robert Hanus
Faculty of Electrical and Computer Engineering
Rzeszów University of Technology
Rzeszów, Poland
rohan@prz.edu.pl

Marcin Zych
Faculty of Energy and Fuels
AGH University of Kraków
Kraków, Poland
zych@agh.edu.pl

Piotr Ochał
Bury Technologies
Rzeszów, Poland
pochal@mail.com

***Abstract*—In this work, the VGG-16 Convolutional Neural Network (CNN) was used for the analysis of spectrogram images of signals obtained from liquid–gas flow using gamma absorption. Four types of water–air flow regimes were studied: plug, slug, bubble, and transitional plug–bubble flow. The experiments were carried out in a laboratory hydraulic installation with a horizontal pipeline equipped with a radiometric measurement system consisting of an Am-241 gamma radiation source and a NaI(Tl) scintillation detector. It was found that the CNN correctly recognized the flow regime in more than 90% of cases.**

Keywords—Two-phase flow, radioisotope method, flow regime recognition, spectrogram, Convolutional Neural Network

I. Introduction

In many branches of industry, such as the mining, nuclear, petrochemical, and energy industries, two-phase liquid–gas flows occur. To control industrial processes, it is important to know the structure of such flows. Currently, computational intelligence methods, such as artificial neural networks and expert systems [1–4], are commonly used for identifying two-phase flow patterns. Various types of sensors are used to acquire data, including capacitive, optical, thermal, radiation, and differential pressure sensors. One of the measurement techniques used, also by the authors of this paper, is the gamma radiation absorption method [5–8].

In machine learning methods, signal features defined in the amplitude, time, and frequency domains are used. In the amplitude domain, amplitude probability distributions [9,10] can be useful; in the time domain, statistical parameters of signals, such as mean value, variance, RMS (Root Mean Square), kurtosis, skewness, and higher-order moments [7,11,12], are utilized. Significant signal features in the frequency domain can be determined, for example, using the Fourier transform, while in the time–frequency and time–scale domains, the STFT (Short-Time Fourier Transform) and wavelet transform are applied [6,13–15].

In recent years, studies of two-phase flows using artificial neural networks have shown growing interest in deep learning methods and the use of convolutional neural networks [16,17]. The input data most commonly consist of flow images obtained using optical methods (high-speed cameras), although images acquired using other measurement techniques can also be used.

In this study, the VGG-16 (Visual Geometry Group) convolutional neural network was used to analyze spectrograms of signals recorded during water–air flow measurements in a horizontal pipeline using the γ-radiation absorption method. The measurement data were recorded at a laboratory test stand for flow studies using radioisotope methods, built at the AGH University of Krakow. The stand allows the simulation of various types of liquid–gas flow, such as plug, slug, transitional plug–bubble, and bubble flow. The OCTAVE software, including its signal processing package, was used to prepare the spectrograms. The TensorFlow library was used to train the neural network with the help of the Google Colab service [18].

II. Two–Phase Flow Measurements Using the Gamma-ray Absorption Technique

The application of gamma radiation absorption in measurements relies on the exponential attenuation of the γ-ray beam, which depends on the absorber's geometric characteristics (such as thickness), its physical properties (including mass and density), and chemical composition [19]. Changes in radiation intensity are recorded by scintillation detectors and converted into electrical pulses (most often voltage pulses). A typical measurement setup for studying two-phase flow by using the γ-radiation absorption method is shown in Fig. 1.

The radioactive source (2), placed on one side of the pipe, emits a γ-radiation beam (3) shaped by a collimator (1). Gamma photons pass through the pipeline with the liquid-gas mixture, undergoing partial absorption. The scintillation detector (5) with the collimator (4) is placed on the opposite side of the pipe, facing the source. At the detector output, electrical pulses $I_x(t)$ are obtained, shaped by the probe's front-end electronics and subsequently recorded by an external data acquisition system. In the presented studies, a radiometric measurement system consisting of an Am-241 linear radiation source with an energy of 59.5 keV and a detector equipped with a NaI(Tl) scintillation crystal was used.

* This work was financed by the Department of Nuclear Energy and Radiochemistry, Faculty of Energy and Fuels, AGH University of Krakow, under grant no. 501.00-210000-10000, and by the Rzeszów University of Technology under grant no. PB22.EM.26.001.

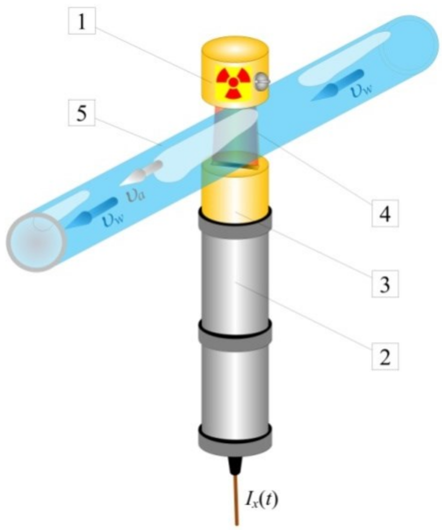

Fig. 1. Schematic diagram illustrating the application of the gamma-ray absorption principle in liquid–gas flow measurements: 1 – source of γ radiation in a collimator, 2 – scintillation probe, 3 – detector collimator, 4 – gamma radiation beam, 5 – pipe, υ_a – velocity of gas, υ_w –velocity of liquid, $I_x(t)$ – voltage pulse signal [10].

III. Laboratory Stand

The γ-absorption measurement set described in Chapter Two was used in laboratory studies of flow using radioisotope methods. An appropriate experimental facility was built at the AGH University of Krakow. A detailed description of the facility is presented in [7,13]. The main part of the hydraulic installation is a horizontal metalplex pipeline, 4.5 m long and with an internal diameter of 30 mm. An overall view of the installation measurement section is shown in Fig. 2.

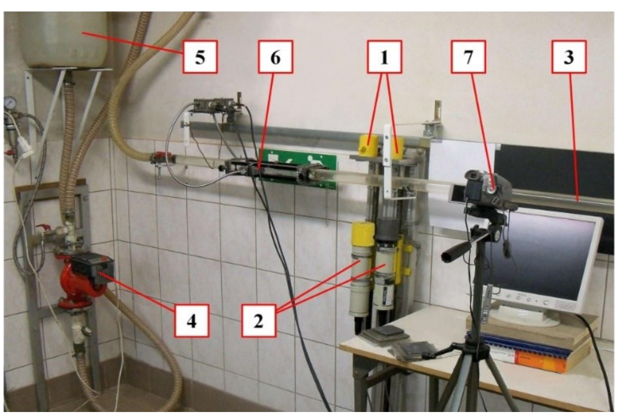

Fig. 2. General view of the hydraulic installation used for two-phase flow measurements: 1 – Am-241 radioactive sources, 2 – NaI(Tl) scintillation detectors, 3 – pipeline, 4 – pump, 5 – expansion tank, 6 – ultrasonic flowmeter, 7 – camera [7].

Figure 3 shows images of representative structures of the analyzed water–air flow types: slug flow (3a), plug flow (3b), plug-bubble flow (3c), and bubble flow (3d). The data acquisition system includes a counter card connected to a PC via a USB port. The voltage pulses $I_x(t)$ were recorded at a sampling frequency of 1 kHz for 3 minutes, resulting in signals $x(t)$ consisting of 180,000 samples. The time courses of the signals for the analyzed flow types, after the centering operation, are shown in Fig. 4.

a)

b)

c)

d)

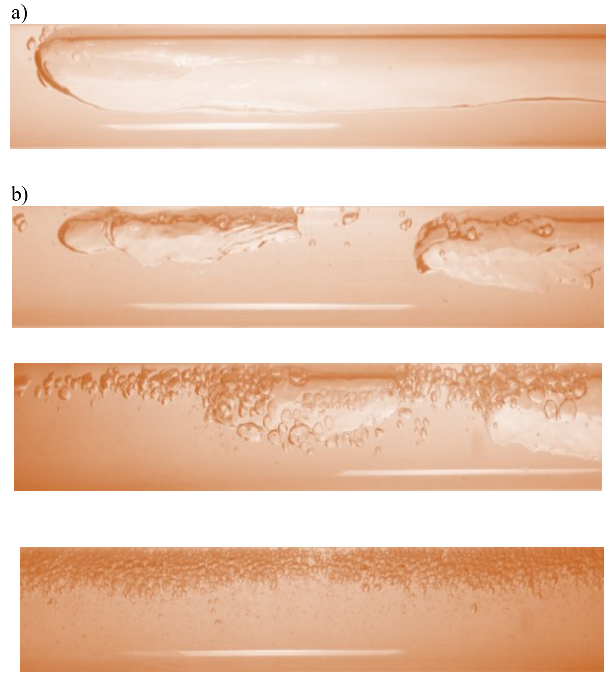

Fig. 3. Photos of structures of water-air flow: (a) slug, (b) plug, (c) plug-bubble, and (d) bubble.

a)

b)

c)

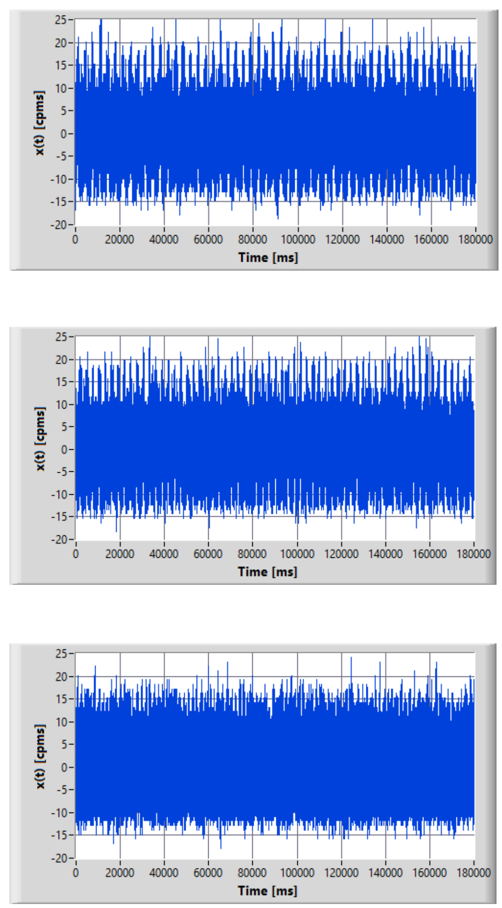

d)

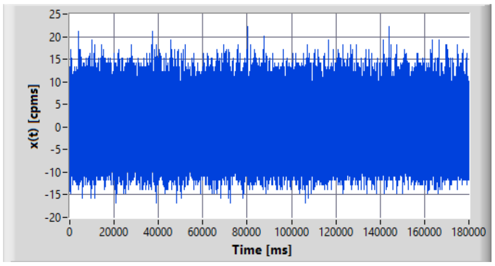

Fig. 4. Recorded signals $x(t)$ for water-air flows: (a) slug, (b) plug, (c) plug-bubble, and (d) bubble.

IV. Convolutional Neural Network

Among various deep learning architectures, the Convolutional Neural Network (CNN) is the most popular for image recognition tasks. This architecture utilizes convolution operations [20]. The CNN architectures most commonly used in studies of two-phase flows are LeNet-5, AlexNet, and VGG-16. These three types of CNNs differ in network depth and filter size. Studies described in [16], concerning two-phase flow structures based on high-speed camera image analysis, showed that the best results were obtained using the VGG-16 network. For this reason, this network architecture was also used in the present work.

For flow-type classification using CNNs, spectrogram images generated from signals acquired by scintillation detectors can be used as predictors. The dataset was created by dividing the probe signals into windows of 20,000 data points with a stride of 10,000 points (50% overlap), from which spectrogram images were generated using STFT. The input images did not contain titles, legends, or axis labels to prevent these elements from negatively affecting the learning process. The STFT parameters, including segment length, window length, and overlap, were selected to obtain spectrogram images with a resolution of 224 × 224 pixels. This resolution corresponds to the default input size required by the VGG-16 convolutional neural network architecture. In this study, spectrograms generated using the Hamming window, shown in Fig. 5, were analyzed.

The network applied for training was a modified VGG-16 network available in the TensorFlow library [18]. This network was originally developed for training using the ImageNet database. The feature combination mode was set to maximum (max-pooling), which reduces computational costs [21].

a) b)

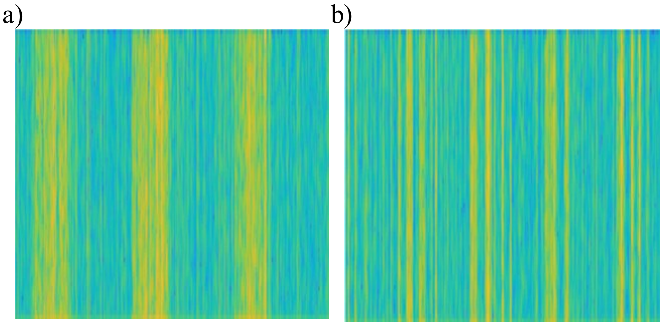

c) d)

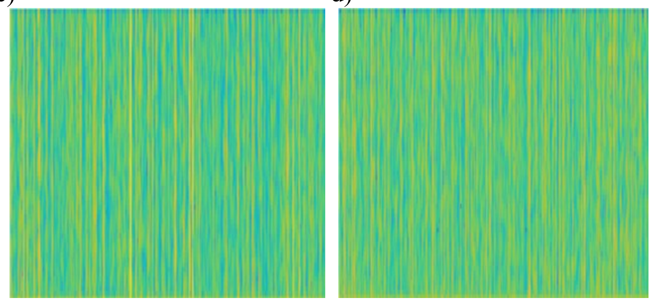

Fig. 5. Examples of spectrograms of $x(t)$ signals for water-air flows regimes: (a) slug, (b) plug, (c) plug-bubble, and (d) bubble.

V. Example Results

The calculations were carried out using the Google Colab service. Transfer learning was not used in this study. The VGG-16 network was initialized with random weights and trained from scratch using the full architecture. No additional dropout or L2 regularization layers were added. The model was trained using the Stochastic Gradient Descent optimizer with Momentum (SGDM) with a learning rate of 0.001 and momentum of 0.95. Based on the performed experiments, the following network parameters were used: maximum number of epochs: 180; batch size (number of data samples analyzed by the network at a given time): 4. The network was trained using spectrogram images obtained with the Hamming window. The dataset was randomly divided into training and testing/validation subsets consisting of 228 and 96 spectrogram images, respectively. Since the spectrograms were generated from signals recorded during the same experimental runs, some statistical dependence between samples may exist. Therefore, the obtained results should be treated as preliminary and will be verified in future studies using independent experimental runs and cross-validation procedures. Based on the test set, the trained network was evaluated and a confusion matrix was plotted (Fig. 6).

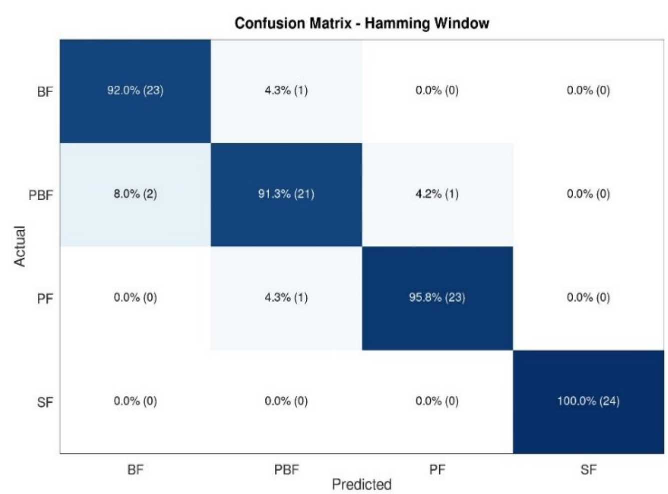

Fig. 6. Confusion matrix for the VGG-16 CNN trained using spectrogram images generated with the Hamming window: BF - bubble flow; PBF - plug-bubble flow; PF - plug flow; SF - slug flow.

Based on the obtained results, the following performance metrics were calculated: accuracy (*Acc*), sensitivity (*Sens*), specificity (*Spec*), precision (*Prec*) and *F1* score, according to [22–25]:

$$Acc = \frac{TP + TN}{TP + FP + TN + FN} \quad (1)$$

$$Sen = \frac{TP}{TP + FN} \quad (2)$$

$$Spec = \frac{TN}{TN + FP} \quad (3)$$

$$\mathrm{Pr}\,ec = \frac{TP}{TP + FP} \quad (4)$$

$$F1 = \frac{2 \cdot TP}{2 \cdot TP + FP + FN} \quad (5)$$

where: *TP* (True Positive) represents elements correctly identified as positive by the model; *FP* (False Positive) represents elements incorrectly identified as positive; *TN* (True Negative) represents elements correctly identified as negative; and *FN* (False Negative) represents elements incorrectly identified as negative.

The obtained results are summarized in Table I. The *F1* score ranges from 0 to 1, where the minimum value is achieved when $TP = 0$ (i.e., when all positive samples are misclassified), while the maximum value occurs when $FN = FP = 0$, corresponding to perfect classification. Two main characteristics distinguish the *F1* score from accuracy: the *F1* score is independent of *TN* and is not symmetric when the classes are interchanged [24]. The obtained *F1* score values are satisfactory in all cases, as all values of this coefficient are greater than 0.8. The best results were achieved for slug flow.

TABLE I. VALUES OF THE INDICATORS

Flow regime	*Acc*	*Sen*	*Spe*	*Prec*	*F1*
slug	1	1	1	1	1
plug	0.979	0.958	0.986	0.958	0.958
plug-bubble	0.948	0.875	0.972	0.913	0.894
bubble	0.969	0.958	0.972	0.920	0.939

The most computationally demanding stage of the proposed method is the CNN training process. The training was performed in a cloud-based environment and required approximately 21 minutes in total, corresponding to an average of 7 seconds per epoch for 180 epochs. However, once the network has been trained, the inference stage requires relatively low computational effort, enabling rapid classification of flow regimes.

VI. CONCLUSION

The article presents the possibility of using the VGG-16 convolutional neural network to identify liquid–gas flow structures in a horizontal pipeline based on the analysis of spectrograms of signals obtained from a radiometric measurement system. Studies were conducted for four flow types: plug, slug, plug–bubble, and bubble. Based on the obtained results, it was found that the VGG-16 CNN correctly recognizes the flow structure in more than 90% of cases.

In radioisotope measurements of two-phase liquid–gas flows, the velocities and volumes of the individual components of the mixture are usually determined using various statistical methods [26,27]. By applying artificial neural networks to the same measurement signals, additional information about the flow structure can be obtained, which is important for monitoring and control of industrial processes.

The novelty of the proposed approach lies not in the CNN architecture itself, but in the application of deep learning methods to spectrograms generated from gamma-ray absorption signals. Compared with optical methods, the proposed technique may be more suitable for industrial environments in which direct visualization of the flow is not feasible.

One limitation of the presented study is the relatively small dataset size and the use of spectrograms generated from laboratory measurements under controlled conditions. Future work will focus on increasing the number of experimental runs, testing other CNN architectures, applying cross-validation procedures, and, if feasible, validating the proposed method under industrial operating conditions.

REFERENCES

[1] P. Aarabi Jeshvaghani, Kh. Rezaee, K. Rezaee, S.A.H. Feghhi, A. Jafari, "Using statistical features and a neural network to predict gas volume fractions independent of flow regime changes", *Flow Meas. Instrum*. 93 (2023), 102430.

[2] C.M. Salgado, S.F. Dam, E.J.A. Puertas, R.W.L. Salgado, "Calculation of volume fractions regardless scale deposition in the oil industry pipelines using feed-forward multilayer perceptron artificial neural network and MCNP6 code", *Appl. Radiat. Isot.* 185(10–11) (2022), 110215.

[3] M. Roshani, G. Phan, R.H. Faraj, N.-H. Phan, G.H. Roshani, B. Nazemi, E. Corniani, E. Nazemi, "Proposing a gamma radiation based intelligent system for simultaneous analyzing and detecting type and amount of petroleum by-products", *Nucl. Eng. Technol*. 53(4), (2021), 1277-1283.

[4] R. Hanus, M. Zych, L. Petryka, D. Świsulski, A. Strzępowicz, "Application of ANN and PCA to two-phase flow evaluation using radioisotopes", *EPJ Web of Conferences* 143, (2017), 02033.

[5] G.H. Roshani, E. Nazemi, F. Shama, M.A. Imani, S. Mohammadi, 'Designing a simple radiometric system to predict void fraction percentage independent of flow pattern using radial basis function", *Metrol. Meas. Syst*. 25(2) (2018), 347–358.

[6] Y. Zhao, B. Qincheng, H. Richa, "Recognition and measurement in the flow pattern and void fraction of gaseliquid two-phase flow in vertical upward pipes using the gamma densitometer", *Appl. Therm. Eng.* 60 (2013), 398-410.

[7] R. Hanus, M. Zych, L. Petryka, M. Jaszczur, P. Hanus, "Signals features extraction in liquid-gas flow measurements using gamma densitometry. Part 1: Time domain", *EPJ Web of Conferences* 114, (2016), 02035.

[8] M. Roshani, M.A. Sattari, P.J.M. Ali, G.H. Roshani, B. Nazemi, E. Corniani, E. Nazemi, "Application of GMDH neural network technique to improve measuring precision of a simplified photon attenuation based two-phase flowmeter", *Flow Meas. Instrum.* 75 (2020), 101804.

[9] W. Liu, X. Lv, S. Jiang, H. Li, H. Zhou, X. Dou, "Two-phase flow pattern identification in horizontal gas–liquid swirling pipe flow by machine learning method", *Ann. Nucl. Energy*, 12 (2022), 109644.

[10] R. Hanus, M. Zych, P. Ochał, M. Augustyn, "Identification of the Structure of Liquid–Gas Flow in a Horizontal Pipeline Using the Gamma-Ray Absorption and a Convolutional Neural Network", *Appl. Sci.* 14(11), 2024, 4854.

[11] R. Hanus, M. Zych, L. Petryka, M. Jaszczur, P. Hanus, "Signals features extraction in liquid-gas flow measurements using gamma densitometry. Part 2: Frequency domain", *EPJ Web of Conferences* 114, (2016), 02036.

[12] A.M. Mayet, et al., "Extraction of time-domain characteristics and selection of effective features using correlation analysis to increase the accuracy of petroleum fluid monitoring systems", *Energies* 15(6) (2022), 1986.

[13] R. Hanus, M. Zych, M. Kusy, G.H. Roshani, E. Nazemi, "Application of selected methods of computational intelligence to recognition of the liquid–gas flow regime in pipeline by use gamma absorption and frequency domain feature extraction", *Measurement* 238 (2024), 115260.

[14] S. Hosseini, A.M. Iliyasu, T. Akilan, A.S. Salama, E. Eftekhari-Zadeh, K. Hirota, "Accurate Flow Regime Classification and Void Fraction Measurement in Two-Phase Flowmeters Using Frequency-Domain Feature Extraction and Neural Networks", *Separations*, 9(7) (2022), 160.

[15] S. Hosseini, O. Taylan, M. Abusurrah, T. Akilan, E. Nazemi, E. Eftekhari-Zadeh, F. Bano, G.H. Roshani, "Application of Wavelet Feature Extraction and Artificial Neural Networks for Improving the Performance of Gas–Liquid Two-Phase Flow Meters Used in Oil and Petrochemical Industries", *Polymers*, 13(21) (2021), 3647.

[16] M. Du, H. Yin, X. Chen, X. Wang, "Oil-in-water two-phase flow pattern identification from experimental snapshots using convolutional neural network", *IEEE Access*, 7 (2018), 6219–6225.

[17] W.L. Salgado, R.S.D.F. Dam, F.S.M.D. Desterro, B.L. da Cruz, A.X.D. Silva, C.M. Salgado, "Application of deep neural network and gamma radiation to monitor the transport of petroleum by-products through polyducts", *Appl. Radiat. Isot*., 200 (2023), 110973.

[18] B. Pang, et al., "Deep Learning With TensorFlow: A Review", *J. Educ. Behav. Stat.,* 45 (2019), 227-248.

[19] G.A. Johansen, P. Jackson, *Radioisotope Gauges for Industrial Process Measurements*, New York: John Wiley & Sons, 2004.

[20] J. Raitoharju, Convolutional neural networks, in: *Deep Learning for Robot Perception and Cognition*, New York: Academic Press, 2022.

[21] A. Zafar, et al., "A Comparison of Pooling Methods for Convolutional Neural Networks", *Appl. Sci.* 12(17) (2022), 8643.

[22] S. Osowski, *Metody i narzędzia eksploracji danych*, (*Methods and tools of data exploration*) Legionowo: Wydawnictwo BTC, 2013. (in Polish)

[23] M. Grandini, E. Bagli, G. Visani, "Metrics for Multi-Class Classification: an Overview", *arXiv:2008.05756*. https://doi.org/10.48550/arXiv.2008.05756

[24] D. Chicco, G. Jurman, "The advantages of the Matthews correlation coefficient (MCC) over F1 score and accuracy in binary classification evaluation", *BMC Genomics* 21(6) (2020).

[25] P. Ochał, M. Augustyn, R. Hanus, M. Zych, „Identyfikacja struktury przepływu ciecz-gaz w rurociągu przy zastosowaniu konwolucyjnej sieci neuronowej i spektrogramów sygnałów radiometrycznych" ("Identification of the structure of liquid-gas flow in a pipeline using a convolutional neural network and spectrograms of radiometric signals") *Przegl. Elektrotech*. 100(7) (2024), 131-134. (in Polish)

[26] R. Hanus, M. Zych, A. Golijanek-Jędrzejczyk, "Investigation of liquid–gas flow in a horizontal pipeline using gamma-ray technique and modified cross-correlation", *Energies* 15(16) (2022), 5848.

[27] R. Hanus, M. Zych, A. Golijanek-Jędrzejczyk, "Measurements of dispersed phase velocity in two-phase flows in pipelines using gamma-absorption technique and phase of the cross-spectral density function", *Energies* 15(24) (2022), 9526.